Transactions, SMiRT-25
Charlotte, NC, USA, August 4-9, 2019
Division V

REINFORCED UNDERGROUND CONCRETE DUCTBANKS AS A BETTER POWER TRANSMISSION ALTERNATIVE TO OVERHEAD POWER LINES IN EARTHQUAKE- AND FIRE-PRONE AREAS

Shakhzod Takhirov[1], Eric Fujisaki[2], Brian Low[3] and Khalid Mosalam[4]

[1] Eng. Manager of Structures Laboratory, Civil and Environmental Engineering Department, University of California, Berkeley; 337 Davis Hall, UC Berkeley, CA 94720
[2] Consulting Civil Engineer, InfraTerra, Inc., 5 Third Street, San Francisco, CA 94103
[3] Principal Civil Engineer, Pacific Gas and Electric, San Ramon, CA 94583
[4] Taisei Professor of Civil Engineering, Director of PEER, Civil and Environmental Engineering Department, University of California, Berkeley; 723 Davis Hall, UC Berkeley, CA 94720

ABSTRACT

Concrete ductbanks are commonly used in many seismic regions throughout the world for power transmission and distribution with the USA and New Zealand being as representative examples. In addition, concrete ductbanks may be employed within a substation, switchyard, or power generation facility for housing medium voltage power cables, control cables, or other circuits. The main purpose of concrete ductbanks is to provide protection for the conveyed cables from environmental (e.g., ground displacement, fire) and mechanical effects (e.g., traffic loading, security, accidental dig-in). Therefore, structural integrity of concrete ductbanks is crucial for ensuring the continued functionality of the conveyed cables. For power transmission cables, uninterrupted power supply to large cities is especially important in providing emergency services after an earthquake and avoiding massive blackouts. These are essential requirements of resilient cities in the face of natural hazards. In a substation, switchyard, or power generation facility, adequate performance of the ductbank helps to ensure continued functionality of the various systems supported by the conveyed cables. The structural integrity can be compromised by many major events, including seismic impact, liquefaction and soil settlement. Based on the experimental research conducted in this study on unreinforced and reinforced ductbanks at the Pacific Earthquake Engineering Research (PEER) Center, UC Berkeley, this paper is focused on an experimental and numerical study of a typical real-life installation. The results of the extensive full-scale testing program conducted on 8-m long concrete ductbanks and their components are used in calibrating the numerical model. The paper demonstrates the advantages of using the undergrounding with the most significant one being an excellent protection from fire initiation including wildfire events. By changing the design of concrete ductbanks from simplified unreinforced concrete covering plastic conduits to well-engineered reinforced concrete configuration, the ductility of the ductbanks and their rotational capacity can be significantly improved. As a result (in addition to the fire protection), the ductbanks can accommodate large ground displacements associated with landslides or significant soil settlement.

INTRODUCTION

The recent massive and deadly wildfires in California, USA have shown that overhead power lines can be a source of the fire because of their vulnerability and possibility of failure under high wind loading. One of the options to address this issue is an installation of underground power lines. Although the underground high-voltage lines are much more costly than overhead lines, they are frequently favoured by the public in highly developed urban areas due to the elimination of visual impacts and electro-magnetic radiation concerns. In the case of transmission lines, different types of underground transmission cables have been installed by utilities and operators. Most new systems use cross-linked polyethylene (XLPE) type cables, which are sometimes directly buried by placing them in trenches back-filled with a cement slurry. In the installation simulated by the experiments described in this paper, the cables are housed in conduits which are then encased in concrete ductbanks, and buried beneath city streets. In addition to cable burial, underground concrete vaults are generally installed at intervals to provide access for pulling and installation of cable splices. In a ductbank installation subjected to large ground displacement, cables may fail by excessive tension or compression, excessive curvature (when minimum bend radius is violated), or crushing or pinching of the cable/conduit. In addition, it is desirable to prevent excessive deformation or damage to the embedded conduits, since a damaged cable may be replaced by pulling a new cable through it in order to return the circuit to service. A conduit that has deformed such that a replacement cable cannot be pulled in, would be considered to have failed. There is very limited experimental information on ductbanks, which was the major motivation to undertake this extensive research. The paper presents a summary of this research with more details to be found in [1-3].

FULL-SCALE EXPERIMENTAL STUDY

The main purpose of the concrete ductbanks is to provide protection for buried high-voltage cables from environmental and mechanical effects. The structural integrity of ductbanks can be compromised by many major events, including seismic effects, liquefaction, and soil settlement. The main subject of the study is to investigate the structural capacity of typical full-scale ductbanks subjected to bending and shear loads. A complete list of full-scale test specimens conducted for this purpose is presented in Table 1.

Table 1: List of full-scale test specimens.

Specimen	Dimensions (m)	Reinforcement	Test method
PGEDB1	8.08×0.78×0.86	No	3 point bending: top loading
PGEDB2	8.08×0.78×0.86	Yes	3 point bending: top loading
PGEDB3	8.13×0.78×0.86	Yes	3 point bending: side loading

Three of the specimens were tested in a three-point-bending test configuration. To account for differences in conduit performance, both 152 mm PVC and HDPE schedule 40 conduits were used in the study and each specimen had a pair of each. The pipe type was consistent with direction of loading and the same type was used on the left and right sides of the ductbank specimens (relative to the loading location). First specimen, PGEDB1, was constructed of unreinforced concrete with embedded conduits. The load at midspan of the ductbank was applied in the strong direction along the depth, in the so-called 'top loading' configuration. Second and third specimens, PGEDB2 and PGEDB3, were constructed of reinforced concrete with embedded conduits and had the same reinforcement design as shown in Figure 1a. The only difference between PGEDB2 and PGEDB3 was the direction of loading: PGEDB2 was loaded in its strong direction along its depth ('top loading' configuration) whereas PGEDB3 was loaded in the specimen's weak direction along its width, in the so-called 'side loading' configuration. Two full-scale specimens, PGEDB4 and PGEDB5, were tested in pure shear loading. These specimens had a single PVC conduit per specimen that spanned across a fully penetrated flat crack through concrete surrounding the conduit. A case of a crack with no gap and a case with a crack with 3 mm opening were introduced in these specimens. Due to the size limitations of the paper, specimens PGEDB4 and PGEDB5 are not discussed herein.

The main objective of the full-scale ductbank tests was to estimate their bending moment and displacement capacities. A typical cross section of the ductbank is presented in Figure 1a. A special experimental setup was designed and assembled for this purpose as presented in Figure 1b. Since the experimental program utilized a three-point-loading test approach, the test setup consisted of two supports at the two ends of the specimen and a hydraulic actuator imposing a load at mid-span. The actuator reacted against a special U-shaped reaction frame designed for the test and attached to the strong floor. The supports under the test specimen were designed as two pillow blocks with cylindrical pins with diameters of 102 mm. One of the pillow blocks was installed on a 76 mm plate rigidly fixed to the strong floor and the other one was installed on an unrestrained 76 mm plate to accommodate the sliding motion of this support along the longitudinal direction of the specimen. To minimize friction effects, the sliding surface at this location was greased. The 76 mm plate had a precisely machined round-shaped shallow groove with the same diameter as that of the pins. To simulate perfect pin condition, both pins were also greased to minimize friction effects due to potential pivoting expected during the test. To prevent slippage of the conduits into test specimens observed during testing of PGEDB1, special fixtures were introduced in specimen PGEDB2 and PGEDB3. Plastic conduits were restrained at the outer ends to minimize their slippage inside of the concrete ductbank.

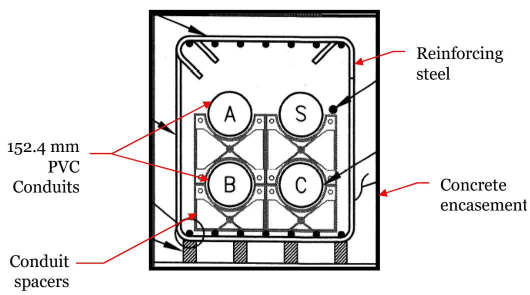

a) Cross section

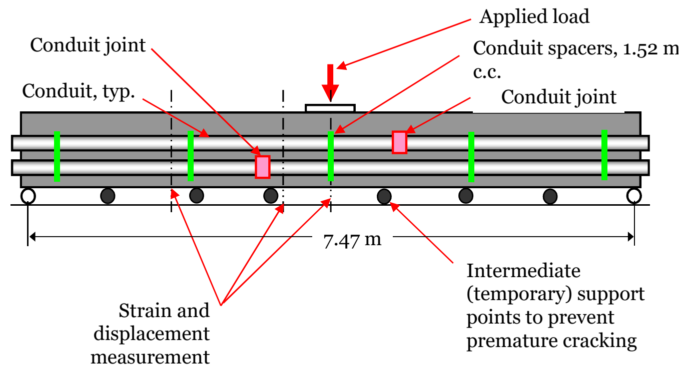

b) Test setup

Figure 1. Typical cross section of a ductbank and schematic drawing of a test setup (conduit spacers were installed at five locations shown in green on the right image).

Unreinforced concrete ductbank under top loading. Prior to the test, PGEDB1 was scanned from many positions to determine as-built geometry of the test specimen [4]. In addition to the scans of the external surfaces of the concrete, the inner surface of the conduits was documented by means of the laser scanner. It was observed that the inner surface is curved upward due to the buoyant force of the fresh concrete during the placing process. To overcome the buoyant force and keep the conduits at the same depth from the surface (that is critical for field installations with long conduits), it is recommended to add weights at the spacer locations.

The force versus displacement plot shown in Figure 2a clearly demonstrates that performance of the unreinforced duckbank was linear up to failure, where the ultimate load before brittle failure was 112.5 kN (point A1 in Figures 2a and b). The ductbank failed in a brittle manner and, consequently, the ductbank split into blocks of unreinforced concrete held together by means of the polymer conduits. Since this brittle performance was expected, the actuator attachment was designed to continue holding these two halves. As a result, about one-third of the total weight of the ductbank, namely -33.1 kN, became suspended from the actuator upon failure of the ductbank as shown in Figure 2a (point A2). This force was negative since it corresponded to tension in the built-in load cell of the actuator. Further increase in actuator displacement after this point engaged some load carrying capacity of the polymer conduits, which reduced the force to about -3.8 kN. After about 215 mm of travel, conduit pipes slipped causing a significant drop in force carrying capacity (point A3 in Figure 2a), which was partially recovered when the actuator was pushed further down as shown in Figure 2a. The final oval shape (referred to as ovality) measurement of the PVC conduit was performed at 178 mm actuator displacement that revealed insignificant ovality of 4.4% in the vicinity of the conduit's mid-span. These performance limits of the PGEDB1 are summarized in Table 2.

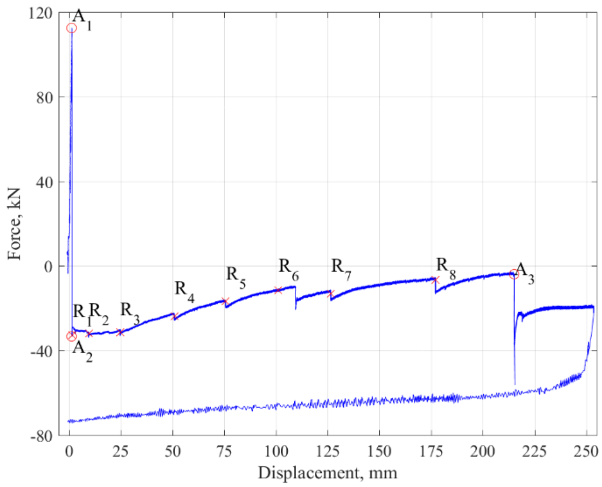

a) Force vs. displacement during the test

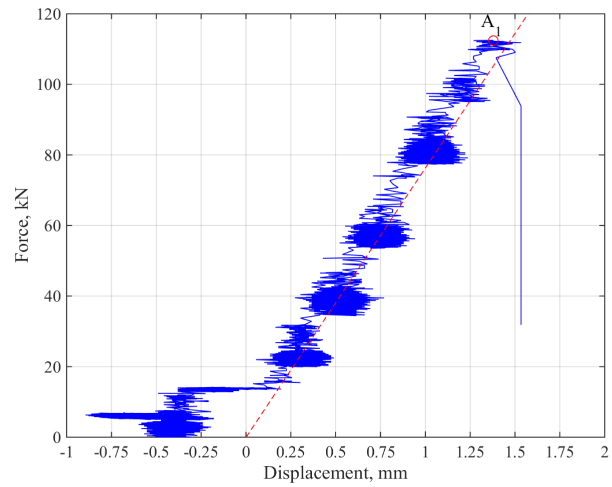

b) Force vs. displacement up to concrete fracture

Figure 2. Force vs deflection diagram for PGEDB1

Failure surface of the ductbank after sawing the polymer conduits is shown in Figure 3a. As it can be seen from the photo, the mid-span spacer was exposed in the failure surface supporting the assumption that the spacer created a weak zone at this location with maximum bending moment. The smooth surface of the plastic spacer most likely compromised the bonding capacity of the concrete at this location creating an effect of a weak vertical plane. A typical spacer consists of two portions. The first portion supports the bottom conduits and the second one keeps the same space between the bottom and top conduits. The spacer exposed in the opening of the crack is shown in Figure 3b. Based on these observations during and after the test, it is recommended to stagger the bottom and top portions of the conduit spacers to minimize the effect of the weak vertical plane that can compromise the bending moment capacity of the ductbank.

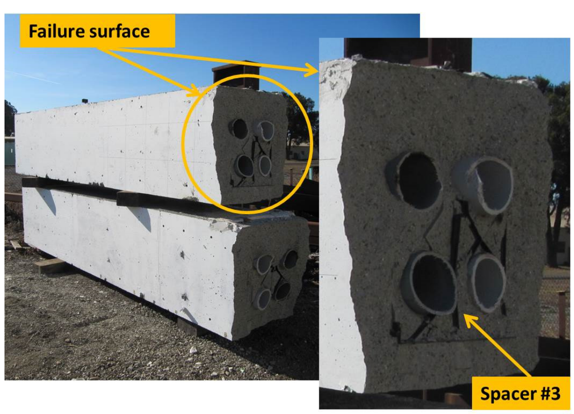

a) Failure surface coincides with location of the spacer at mid-span

b) View into the crack exposing the spacer (black pieces)

Figure 3. Failure mode of unreinforced ductbank (PGEDB1)

In addition to the laser scanning, a special non-destructive inspection equipment was used to locate and measure the ovality of the 152 mm PVC conduit encased in the concrete while the ductbank was subjected to incrementally increasing deflections (they are noted by R1 through R8 in Figure 3a). The pipe's inner surface was inspected with Rovver 400 [5], a remotely operated video inspection vehicle, outfitted with a laser ring measuring system to provide a live-stream video signal showing a 360 degree laser ring projected on the pipe's inner surface. The video signal was reduced in a special software package [5] to take measurements of the conduit features affected by the external forces deforming the pipe. A pipe on the tension side of the ductbank was selected for the inspections. Before start of the test, the whole pipe segment was documented for imperfections to create a video baseline. Subsequently, the pipe's inner surface was documented with the laser ring system at several loading levels during the test. Measurements were taken at locations where signs of deformation or failure showed on the pipe's inner surface to measure the severity of ovality or deformation.

The ovality inspections for PGEDB1 were conducted at several deflections of the ductbank with the final one conducted at 178 mm displacement. The maximum change of the pipe diameter in the vertical direction did not exceed 4.4% which was measured at mid-span of the PVC conduit and difficult to detect by a naked eye as presented in Figure 4a. No cracks were observed in the joint as shown in Figure 4b.

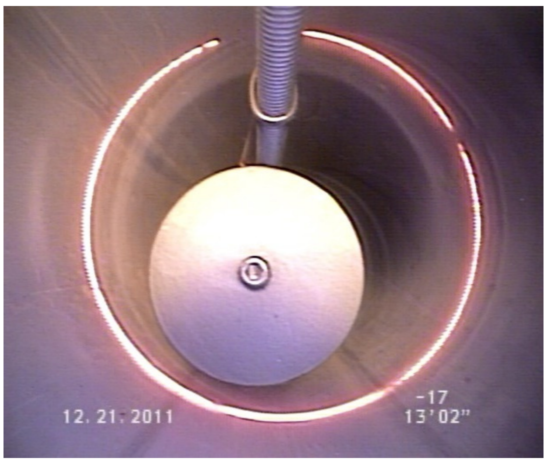

a) Inner surface of PVC pipe in vicinity of mid-span with the largest ovality (178 mm displacement)

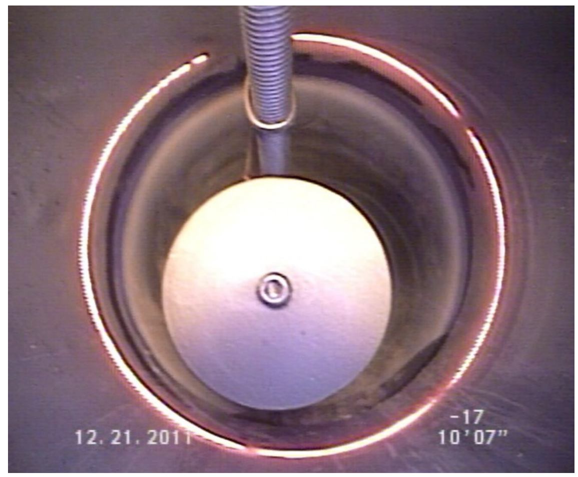

b) Inner surface of PVC pipe at the joint – 914 mm away from mid-span (178 mm displacement)

Figure 4. Insignificant ovality of PVC pipe with no visible cracks at joint location (PGEDB1)

It is worth noting that in many cases the clearance between the conduit's inner surface and the power cable was large enough to accommodate ovality up to 25%. Therefore, although the structural integrity of the unreinforced ductbank was compromised and it broke into two concrete blocks, the pinching of the power cable most likely would have not occurred until at least 178 mm mid-span displacement, i.e. about 2.4% of the span length. However, the conduits in case of PGEDB1 were not restrained at the ends against slipping and in case they were restrained, larger ovality could have occurred for the conduits.

Reinforced concrete ductbank under top and side loading. As opposed to PGEDB1, the reinforced ductbanks demonstrated ductile performance as expected. A photo of the test specimen during the test is presented in Figure 5a. The cracking pattern was distributed along the longitudinal direction as it was expected for reinforced concrete beams. The loading was paused several times during the test to measure ovality of the conduits by sending the remotely operated video inspection vehicle inside the pipe and pulling through a mandrel which simulated pulling a cable through the conduit. In addition to that, laser scans of the test specimen were performed during these pauses. It is to be noted that the pauses were long enough to introduce some force relaxation in the specimen (Figure 5b), since the actuator was operated in displacement control.

The ductbank's load carrying capacity was steadily increasing up to 188.8 mm displacement when the ultimate load of 532.2 kN was observed as presented in Figure 5b (point B1). The load carrying capacity of the ductbank slightly decreased after that but remained somewhat stable up to 284 mm displacement when one of the reinforcing bars fractured as shown in Figure 6b. At this point, the force dropped from 524.3 kN to 493.0 kN (point B2 in the plot). The specimen picked up some force when the actuator continued pushing it down until second reinforcing bar failed at 308.4 mm displacement, causing the force to drop from 492.9 to 405.0 kN (noted as B3 in the plot). The force stabilized at about 427 kN when the actuator continued pushing it down until third reinforcing bar failed at about 332.8 mm, with a corresponding force drop from 422.9 kN to 333.8 kN, after which the force increased to about 356.0 kN with continued loading. At 343.4 mm displacement, the test was paused for the final time. Subsequent loading of the specimen exceeded the travel limit of the test setup at 361 mm, which caused a steady increase of force (point B5 in the plot). At this instant, the test was stopped and the actuator was retracted to its starting point.

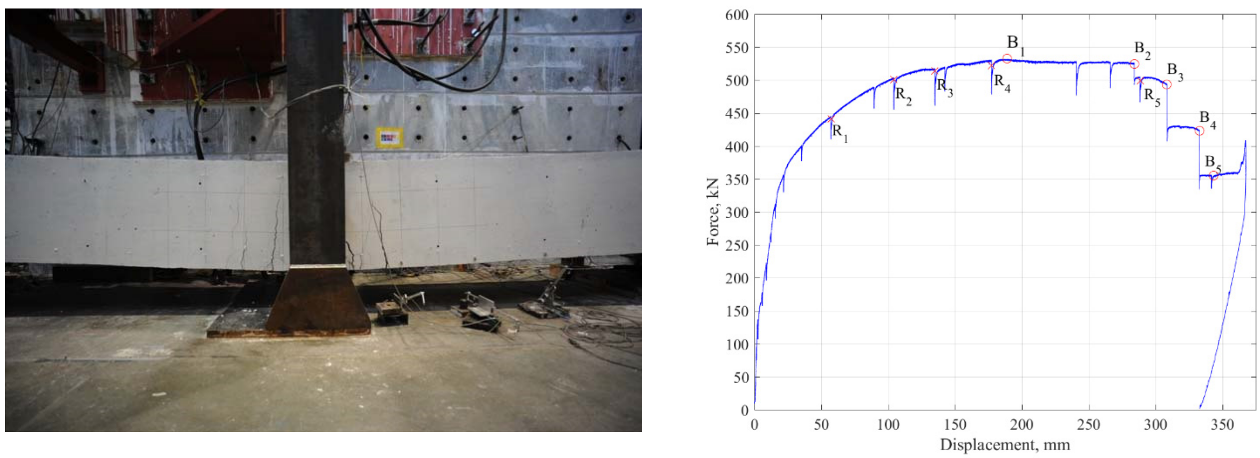

a) Specimen at 290 mm mid-span deflection

b) Actuator force versus mid-span deflection

Figure 5. Structural performance of PGEDB2

The ovality and conduit integrity checks were performed by the rover inside the bottom PVC conduit at different stages of testing. Since the HDPE pipe did not have a joint, only PVC pipes with a joint were investigated by the rover. A wooden mandrel was used to check the ovality of the HDPE pipes. The rover was deployed at 57.3 mm (R1), 104.3 mm (R2), 135.0 mm (R3), 177.3 mm (R4), and 288.3 mm (R5) and compared to that at 0 mm displacement. Although no significant ovality was observed and the rover and the mandrel were able to pass through the conduit, a failure in the PVC joint was observed. It took place between the rover investigations at 177.3 mm (point R4 in Figure 5b) and 288.3 mm (point R5 in the same figure) as presented in Figure 6. All specimens had a sleeve joint in PVC conduit at the same distance from mid-span. It is important to note that the boundary conditions on the conduit were changed for PGEDB2 from free to slip (PGEDB1) to fully restrained leading to excessive tensile strains in the PVC conduit causing failure of the PVC's sleeve joint.

The performance of PGEDB3 specimen was somewhat similar to that of PGEDB2, although its load capacity was much lower. A photo of the test specimen during the test is presented in Figure 7a. A plot in Figure 7b shows force versus mid-span displacement. The cracking pattern was distributed along the longitudinal direction as it was expected for reinforced concrete beams. Similar to the case of PGEDB2, the loading was paused several times during the test to measure ovality of the conduits by sending the rover inside the pipe and pulling through a mandrel. Similar to the other specimens, laser scans of the test specimen were performed during these pauses. The ductbank's load carrying capacity was steadily increasing up to about 135 mm displacement when the ultimate load of 453.9 kN was observed as presented in Figure 7b. The load carrying capacity of the ductbank slightly decreased after that but remained somewhat stable up to about 295 mm displacement when one of the reinforcing bars fractured as shown in

Figure 7b. At this point the force dropped from 429.9 kN to 344.4 kN. The specimen picked up some force when the actuator continued pushing it down until a second reinforcing bar failed at 328 mm displacement, causing the force to drop to 284.8 kN. The force steadily increased after this point to 324.9 kN. At 404 mm displacement, the test was paused and final geometry check was performed. Subsequent loading of the specimen exceeded the travel limit of the test setup at 420 mm, which caused a steady increase of force. At this instant, the test was stopped and the actuator was retracted to its starting point.

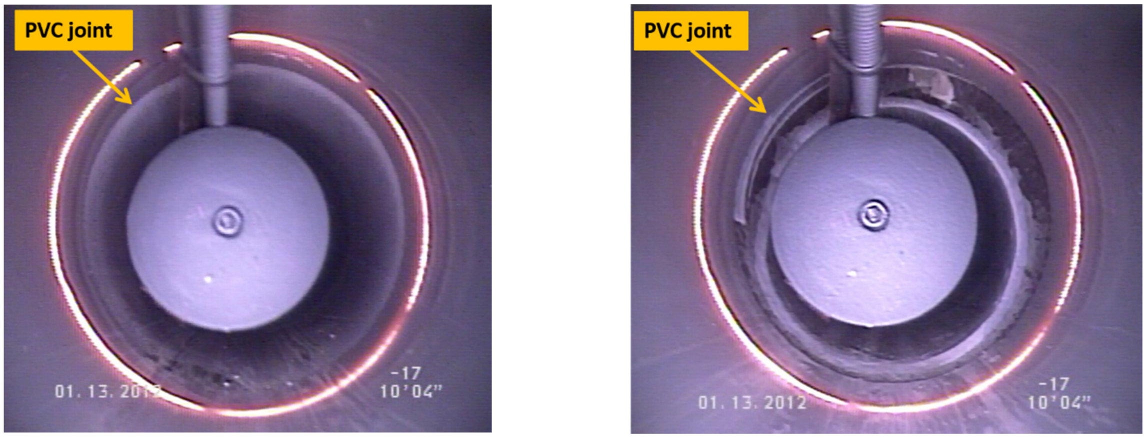

a) PVC joint before failure (at R_4 stage – 177.3 mm)

b) PVC joint after failure (at R_5 stage – 288.3 mm): both rover and mandrel were able to pass through

Figure 6. Inner surface of the polymer conduit before and after failure of sleeve joint of PGEDB2

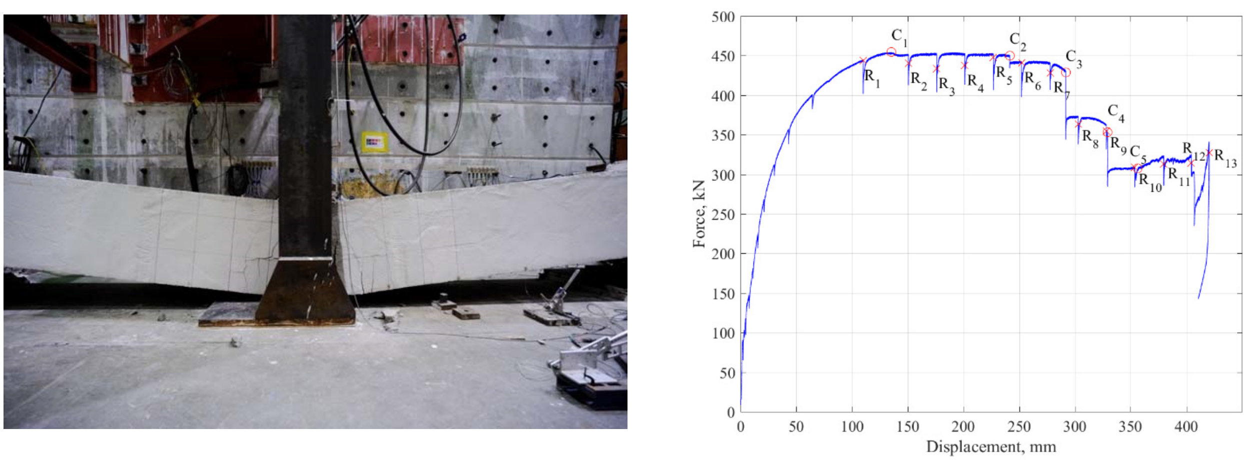

a) Specimen at 419 mm mid-span deflection

b) Actuator force versus mid-span deflection

Figure 7. Structural performance of PGEDB3

The ovality of the inner surfaces of the conduits was documented by the rover. A wooden mandrel was pushed through the conduit to check for ovality of the conduits and make sure that the cable would still pass through the conduit. Although ends of the PVC conduits were restrained, the restraint was not strong enough to prevent slipping in of the bottom PVC pipe. As a result, an insignificant ovality was measured by the rover and no failures in the PVC joint were observed as presented in Figure 8.

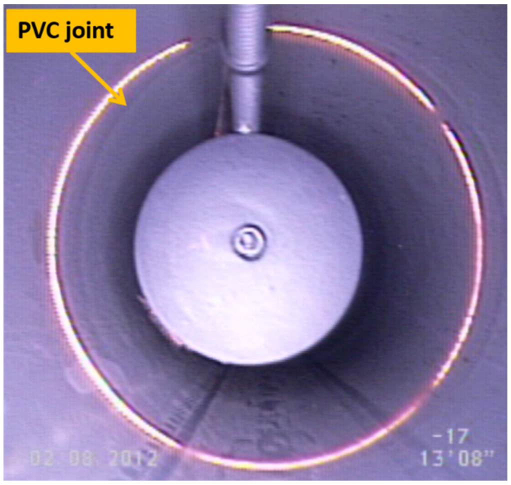

a) PVC joint at zero load

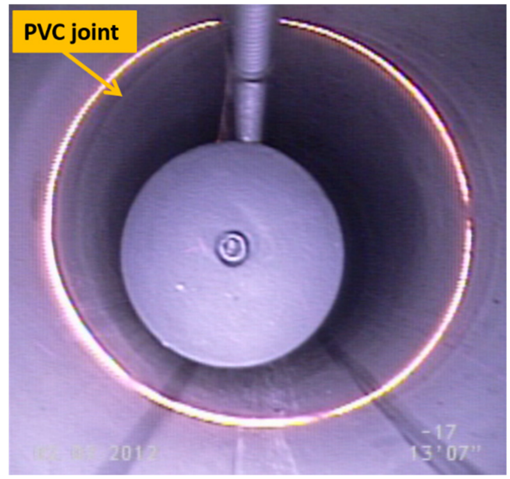

b) No failure at PVC joint (at R_{13} stage – 420.5mm): maximum ovality is 4.2%

Figure 8. Inner surface of the polymer conduit for PGEDB3

FINITE ELEMENT MODELING OF DUCTBANKS

Pipes. Pipes were modelled as linear elastic perfectly plastic, making use of the measured material parameters for PVC and well-known material parameters for HDPE [6]. The properties of HDPE pipe's material were updated based on the results of the bare pipe component tests.

Concrete. Concrete is treated as linear up to a specified level of tensile strain; a crack is then simulated by modifying the constitutive properties (Smeared cracking). When the combination of stresses satisfies a specified criterion, e.g. strain energy reaches some threshold value that corresponds to that of the one dimensional case for the concrete capacity, a crack is initiated. This implies that at the integration points where the stress, strain, and history variables are monitored, the isotropic stress–strain relationship is replaced by an orthotropic elasticity-type relationship.

Steel reinforcement. For the reinforcing steel, a linear elastic perfectly plastic material model with the well-known parameters for a Grade 60 reinforcement steel has been used to start the modelling, then a calibration was performed to match the behaviour of the specimens for large deformations.

The finite element modelling was performed in the general-purpose finite element program DIANA [7]. The experimental force versus displacement curves compared to those of the finite element models are presented in Figure 9. The plots show that there is an adequate correlation between the performance of the actual test specimens and that of the finite element models.

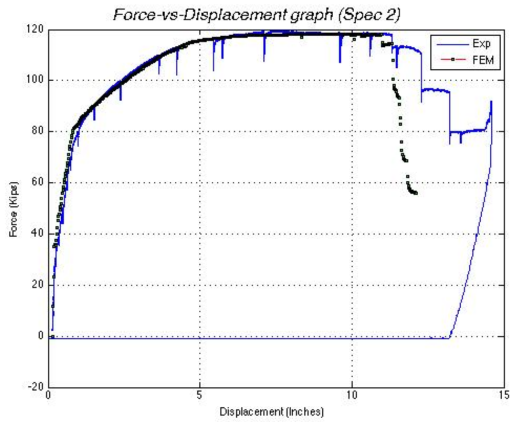

a) PGEDB2

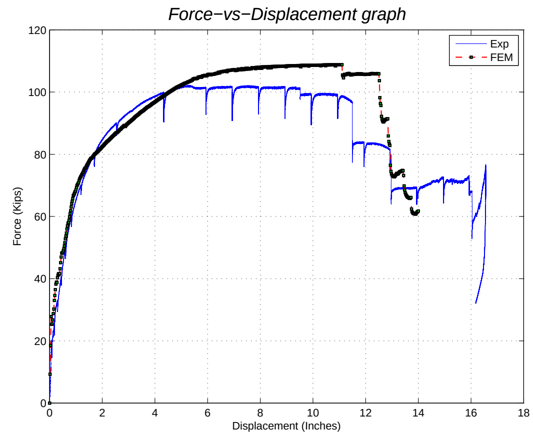

b) PGEDB3

Figure 9. Force versus displacement curves compared to those of FE models (1 kip = 4.45 kN and 1 in = 25.4 mm).

CONCLUSIONS

The study demonstrated that unreinforced ductbanks do not provide a reliable means of cable protection where large deformations of the surrounding soil are expected. A moderately reinforced ductbank is effective in protecting the cables and embedded conduits as demonstrated by acceptable conduit deformation even at high curvature of the ductbank. Since the ductbank's structural integrity can be compromised by many major events, including seismic effects, liquefaction, and soil settlement, the reinforcement design should take into account the displacement demand at the site. Sufficient shear reinforcement of the ductbank should be provided to prevent shear effects for which the PVC conduits have limited capability to accommodate.

The following general conclusions were made:

1. To avoid curving effect due to buoyant force during concrete placing process and to keep the conduits at designated elevation along its length, adding weights at the bottom of the conduit supports is recommended.

2. Since plastic spacers embedded into unreinforced ductback have a strong potential of developing a surface susceptible to failure along the spacer's plane, it is recommended to stagger the spacers' top and bottom parts along the conduit.

3. Since the compression forces in the conduits are limited by small compressibility of the concrete, the tension forces control the structural performance of the conduits. Full-scale testing of the ductbank specimens without restrained PVC pipes showed that allowing slippage of the conduits results in a significantly better performance without failure. Thus, flexible joints enabling expansion in tension are recommended.

4. The FEMs are sufficiently accurate to help develop estimates of curvature limits for reinforced concrete ductbanks.

ACKNOWLEDGMENTS

The authors acknowledge the financial support provided by Pacific Gas and Electric Company, San Ramon, CA. Special thanks are due to Underground Construction Company, Benicia, CA for constructing the test specimens and Pacific Gas and Electric Company for providing robotic rover utilized during the tests. The ovality measurements were conducted by Mr. Robert de Haas of Technical & Ecological Services, NDE - Inspection Services and his effort is greatly acknowledged. The active involvement in the discussions of the test setups and specimens of Mr. Henry Ho of Pacific Gas and Electric Company is greatly appreciated. The authors greatly appreciate participation of Mr. John Schroeder of Pacific Gas and Electric Company in discussions and testing of test specimens. Thanks are due to staff of the Pacific Earthquake Engineering Research Center for performing this extensive experimental program in a timely manner. Special thanks due to Mr. Lev Stepanov of the University of California, Berkeley for his help with concrete cylinder tests. The authors would like to acknowledge Nicolas Peralta for developing FE model id DIANA and performing numerical simulations. The special thanks are due to Dr. Siddaiah Yarra for his help during the tests.

REFERENCES

[1] Fujisaki, E., Takhirov, S. (2013). Seismic Performance of Concrete Ductbanks for Buried Transmission Cables, Workshop on Electric System Earthquake Engineering, University of California, Berkeley, California, USA, April 18, 2013.
[2] Mosalam, K., Takhirov, S., Fujisaki, E. (2012). Seismic Performance of Concrete Ductbanks for Buried Transmission Cables: Full-scale Tests and FE Modeling. Mini-Symposium on Hybrid Simulation: Theory and Applications, University of Minho, Guimarães, Portugal, October 1-4, 2012.
[3] Takhirov, S., Mosalam, K., Yarra S., Peralta N., Fujisaki E. and Ho H. (2013) Full-scale Experimental and Numerical Study of Concrete Ductbanks and Assessment of their Seismic Vulnerability, Proceedings of the SE-50EEE, International Conference on Earthquake Engineering, 29-31 May, 2013, Skopje, Republic of Macedonia.
[4] Khalid M. Mosalam, Shakhzod M. Takhirov, and Sangjoon Park. (2014). 'Applications of Laser Scanning to Structures in Laboratory Tests and Field Surveys'. Journal of Structural Control and Health Monitoring. Volume 21, Issue 1, pages 115–134, January 2014.
[5] http://www.ge-mcs.com/download/RVI/Rovver%20400/rovvermanual.pdf. ROVVER5.0. Pipeline Video Inspection Systems. Maintenance & Operation Manual. Version 8/20/03.
[6] JM Eagle (2011). Electrical Conduit and Duct.
[7] DIANA (2008). Finite Element Analysis User's Manual 9.3, TNO DIANA BV, The Netherlands.